Development of multi-physics multi-scale modelling platform for CFRP composites using inductive thermography techniques.

Abdoulaye BA [1], Bengisu YILMAZ [2], Huu Kien BUI [1] ,Elena JASIUNIENE [2], Gerard BERTHIAU [1]
[1] IREENA and NDTonAIR, Saint Nazaire, France
[2] Kaunas University of Technology and NDTonAIR, Kaunas, Lithuania
Contact e-mail: abdoulaye.ba@etu.univ-nantes.fr

Abstract. Due to their excellent mechanical performance, the use of carbon fiber composites has been growing in recent decades. However, the large-scale development of these materials depends on the improvements of the processes during the various stages of their whole life cycle (producing, forming, assembly, inspection, recycling). At various stages of the life cycle of the material, non-destructive testing (NDT) methods can be used to characterize the health state of the material. They play a vital role in the quality control and risk management. The Induction Thermography is significantly promising NDT technique for inspection of composites and it based on the measurement of eddy current thermal effects. The development of these methods requires multiphysics electromagnetic – thermal modelling. The developed models will deal with some numerical issues concerning thin regions of strong anisotropy and the multiscale geometries. In this paper, we develop a FEM coupled electromagnetic-thermal model in order to investigate the detectability of metal foil incorporate on the interface of three layer composite-adhesive bond.

Introduction

During the manufacturing process or operation time, several flaws can occur in the composites materials. These defects can reduce the mechanical strength and increase the failure risk[1]. In aerospace, composites materials replace metals in structural components due to their light weight and excellent configurable mechanical properties. Adhesive bonding of composites is a new and efficient technology with weight and homogenous load advantages compared to other joining techniques for composites. The imperfections such as porosity, delamination, fiber rupture and contamination are the most encountered flaw types in adhesive bonds. These flaws are considered in mesoscopic scale, i.e. the elementary ply scale. In this work, we use non-destructive testing to investigate the detectability of metal foil incorporate on the interface of three layer composite-adhesive bond numerically[2]. 3D multi-physics and multi-scale modeling approach with Finite Element Method is used.

1. Induction Thermography Technique

Fig. 1 shows our experimental device of the induction thermography techniques. The specimen is heated due to joule effect of eddy-current by a circular coil which is fed by an induction generator via an impedance adaptation circuit. The temperature exposed to the surface of the specimen is then measured with an infrared thermal camera. The presence of defects can disturb the induced currents flow and generate intensified current areas or inhibit the heat diffusion in the composite.

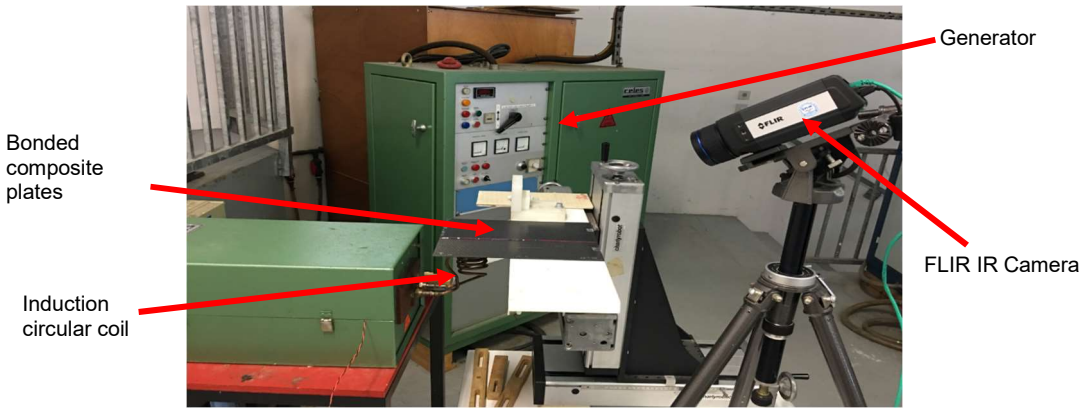

Figure 1: Induction thermography setup

In order to detect and characterize the defects, the temporal evolution of the temperature on the surface of the specimen is processed and analysed. The informations of the coil which we use is shown in Tab. 1.

Table 1: Dimensions of the coil

External Radius	Rext (mm)	12.5
Internal Radius	Rint (mm)	7.5
Number of Turns	N_Turn	5
Height	H (mm)	30

Fig. 3 shows the description of the model that we simulate and experiment with its dimensions.

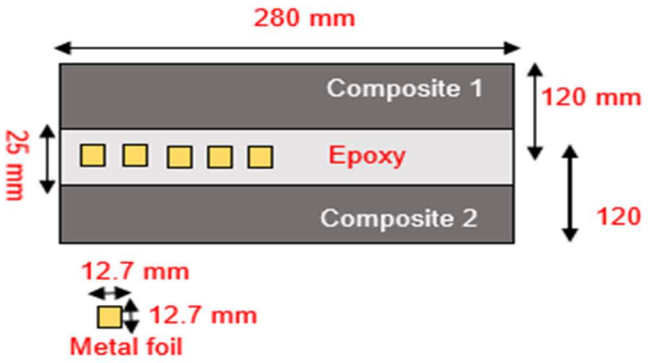

Figure 2: Description of the model. Defects are Metal foils

In this study, we simulate two composite rectangular plates 120mm*280mm bonded together with 25mm bondline with epoxy AF163. The thickness of metal foil is about 0.2413mm. the distance between two metal foil is 15mm. Each composite plate has a thickness of 2.2 mm. The two composite plates have 6 plies of 5H Satin (090) textile. The

purpose of the simulation is to detect defects artificial metal foil defects on the interface of the bonded structure by using induction thermography.

Numerical models permit us a better understanding of defects behaviors and are a very useful for a parametric study. In this study, the goal is to focus much power over the metal foil. To do this, we will make an optimization of the electromagnetic frequency in order to choose the frequency which gives the best ratio power over the metal foil by total power injected (composite plates, metal foil). As the infrared camera records the temporal evolution of the temperature at the upper face, we do also the ratio of power in the metal foil by total power on the top composite plate.

2. Numerical modelling

Induction thermography simulation model involves a coupled electromagnetic and thermal problem[3][4]. Weak electromagnetic $\mathbf{A}-\varphi$ and nodal thermal formulations are used to calculate the eddy currents and temperature distribution on the surface of the specimen.

2.1 Electromagnetic model

The electromagnetic problem can be described as shown in fig. 3. We consider a bounded domain $D=D_{nc} \cup D_c$ with boundary $\Gamma = \Gamma_B \cup \Gamma_H$. The conducting and non-conducting parts of D are denoted by D_c and D_{nc}. The conducting domain is composed of inductor domain and loads domain.

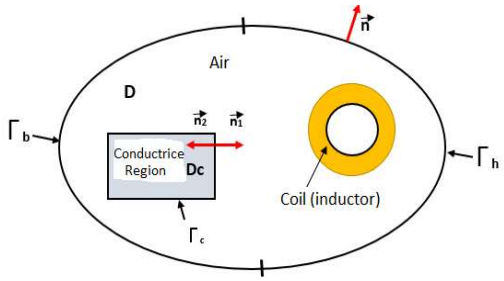

Figure 3: Studied domain

Weak electromagnetic formulation is given by [3][5]:

$$\int_D \left(\mathbf{curl}\left(w_a \frac{1}{[\mu]} \mathbf{curl}(\mathbf{A}) \right) + jw[\sigma] w_a (\mathbf{A} + \mathbf{grad}\varphi) \right) d\Omega - \int_\Gamma w_a \left(n \wedge \frac{1}{[\mu]} \mathbf{curl}(A) \right) = \int_D w_a \mathbf{curl}(\mathbf{T_s}) d\Omega \quad \text{(Eq. 1)}$$

$$\int_{Dc} (jw[\sigma] \mathbf{grad} \mathrm{w_n} (A + \mathbf{grad}\varphi))\, d\Omega = 0 \quad \text{(Eq. 2)}$$

Where $\mathbf{A}$ and φ are respectively the magnetic vector potential and the primitive in time of electric scalar potential. w_a and w_n are respectively denoted edge shape function and nodal shape function [6]. $[\sigma]$ represent the electrical conductivity of the pli i having a fiber orientation θ^i. The matrix form of the discrete $\mathbf{A}-\varphi$ formulation reads :

$$\begin{pmatrix} \mathbf{R}^t M_{ff}^{1/[\mu]} \mathbf{R} + jw M_{aa}^{[\sigma]} & jw M_{aa}^{[\sigma]} \mathbf{G} \\ jw \mathbf{G}^t M_{aa}^{[\sigma]} & \mathbf{G}^t M_{aa}^{[\sigma]} \mathbf{G} \end{pmatrix} \begin{pmatrix} \mathbf{A_a} \\ \Phi_n \end{pmatrix} = \begin{pmatrix} \mathbf{R} M_{ad} T_a^s \\ 0 \end{pmatrix} \quad \text{(Eq. 3)}$$

Where **R**, **G** are respectively the discrete counterparts of rot and grad operators $M_{ff}^{1/[\mu]}$, $M_{aa}^{[\sigma]}$ and M_{aa} are denoted mass matrix. They are given by:

$$M_{ff}^{1/[\mu]}(i,j) = \sum_{i,j=1\dots F} \int_{Dc} \frac{1}{[\mu]} w_f^i w_f^j d\Omega \quad \text{(Eq. 4)}$$

$$M_{aa}^{[\sigma]}(i,j) = \sum_{i,j=1\dots A} \int_{Dc} [\sigma] w_a^i w_a^j d\Omega \quad \text{(Eq. 5)}$$

$$M_{aa}(i,j) = \sum_{i,j=1\dots A} \int_{Dc} w_a^i w_a^j d\Omega \quad \text{(Eq. 6)}$$

2.2 Thermal model

The eddy current losses in the specimen whose volumic power in each element i of the volume mesh can be determined by:

$$P = \mathbf{J}_{ind}{}^{t} \cdot [\sigma]^{-1} \cdot \mathbf{J}_{ind} \quad \text{(Eq. 7)}$$

Eq. 4 represent the heat source of the thermal problem. The latter is defined by:

$$\rho C_P \frac{\delta \mathbf{T}}{\delta t} + div(-[\lambda]\mathbf{gradT}) = P \quad \text{(Eq. 8)}$$

Where T is the temperature, C_P is the specific heat, ρ is the specific mass and $[\lambda]$ is the tensor of thermal conductivities. $[\lambda]$ takes the same form than the electric conductivities $[\sigma]$. In thermal problem only the composite domain is considered.
We consider only the load domain in the thermal problem. So, weak formulation of thermal problem is given by:

$$\int_{Dc} \left(\rho C_P \frac{\delta \mathbf{T}}{\delta t} - div([\lambda]\mathbf{gradT}) \right) w_n d\Omega = \int_{Dc} P w_n d\Omega \quad \text{(Eq. 9)}$$

The matrix form of thermal weak formulation reads:

$$(\mathrm{M}_{nn}^{[\rho c]} + \mathbf{G}^t M_{aa}^{[\lambda]} \mathbf{G} + M_{nn}^{[h]}) \Delta T_{n,i+1} = M_n^{[P]} + M_{nn}^{[\rho c]} \Delta T_{n,i} \quad \text{(Eq. 10)}$$

Where $\Delta T_{n,i}$ is the temperature rise on the n at the instant i with respect to the initial temperature. The matrix $\mathrm{M}_{nn}^{[\rho c]}$, $M_{ee}^{[\lambda]}$, $M_{nn}^{[h]}$ and $M_n^{[P]}$ are given by [7]:

$$\mathrm{M}_{nn}^{[\rho c]}(i,j) = \sum_{i,j=1\dots N} \int_{Dc} \frac{\rho C_p}{\Delta t} w^{ni} w^{nj} dD \quad \text{(Eq. 11)}$$

$$M_{aa}^{[\lambda]}(i,j) = \sum_{i,j=1\dots A} \int_{Dc} [\lambda]\, w^{ni} w^{nj} dD \quad \text{(Eq. 12)}$$

$$M_{nn}^{[h]}(i,j) = \sum_{i,j=1\dots N} \int_{Dc} h\, w^{ni} w^{nj} dD \quad \text{(Eq. 13)}$$

$$M_n^{[P]}(i,j) = \sum_{i=1\dots N} \int_{Dc} P\, w^{ni} dD \quad \text{(Eq. 14)}$$

Δt is the time step and is fixe. The parameters h takes into account the natural convection and the radiation on the surface of the plate.

3. Simulation investigations

Nondestructive testing by induction thermography through adhesive bonding have been simulated using our laboratory Finite Element code. Simulation tests were made with a circular coil where the informations are recorded in the Tab. 1.

In table 2, 3 and 4, we present the numerical parameters of the thermal problem. We have numerical parameters of: composite plates, Epoxy and defects.

Table 2: Thermal parameters of composites

Parameter	Value	Unit
ρ	1599	kg/m^3
C_p	930	$J/(kgK)$
$\lambda_{\|\|}$	4.6	$W/(mK)$
$\lambda_{\perp}$	4.6	$W/(mK)$
λ_z	0.5	$W/(mK)$
$h=h_{conv}+h_{radi}$	10	$Wm^2K)$

Table 3: Thermal parameters of Epoxy

Parameter	Value	Unit
ρ	1215.8	kg/m^3
C_p	1000	$J/(kgK)$
λ	0.1661	$W/(mK)$

Table 4: Thermal parameters of defects

Parameter	Value	Unit
ρ	8500	kg/m^3
C_p	375	$J/(kgK)$
λ	109	$W/(mK)$

The table 5 shows the parameters of the electromagnetic problem.

Table 5: Electromagnetic parameters

Parameter	Value	Unit
$\sigma_{\|\|}$	4×10^4	S/m
$\sigma_{\perp}$	4×10^4	S/m
σ_z	8	S/m
σ_{def}	16.69×10^6	S/m

The parameters in the table 6 have been chosen in the simulation.

Table 6: Simulation parameters

Parameter	Value	Unit
Frequency	$[2\times 10^3 ; 2\times 10^6]$	Hz
Current	200	A
Lift off	2	mm

The mesh used in the simulation is shown in fig. 4. The simulation results are shown in the figure 5. The curves were plotted on a logarithmic scale.

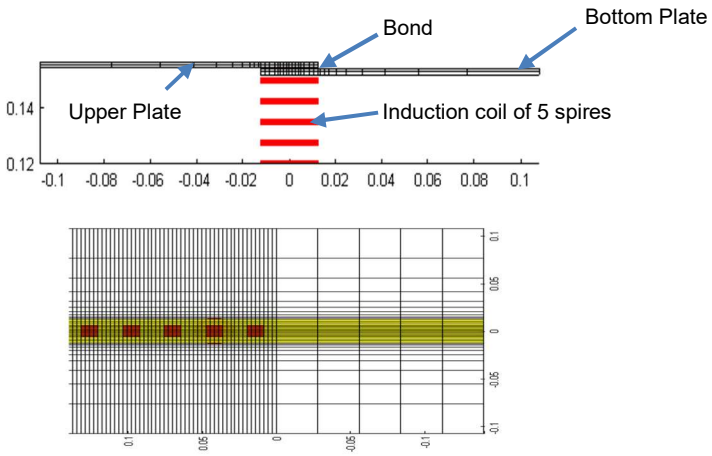

Figure 4: Mesh in the simulation

The circular inductor is placed below the second defect from the middle of the samples. We have five (5) defects in the sample. But only one defect will be inspected. The rectangular red color in the fig. 4 are the defects and the circular one is the coil.

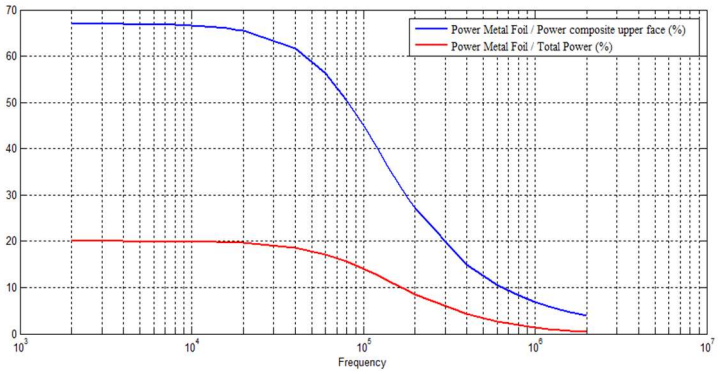

Figure 5: Ration of powers in the metal foil and composites

Fig. 5 shown that from 2 kHz to 40 kHz we have a good ratio for the two cases. For the first one, the ratio is about 70 percent and 20 percent for the second one. For all frequencies between 2 kHz and 40 kHz, we get a good ratio. We choose the frequency of **20 kHz** in order to get a good ratio of powers, in the following. At frequency 20 kHz with an excitation current 200 A, we observe that the powers are too small in each layers.

Since the powers are too small, we increase the current. The latter is chosen ten times larger i.e. 2000A. After simulation, the power in the metal foil goes from 0.08 W (200 A) to 8 W (2000 A) and the total power from 0.3995 W to 39.95 W. In this case, the power of the metal foil is greater than the powers of the upper layers, on the observation side of the infrared camera. The fig. 6 shown the powers in each layers.

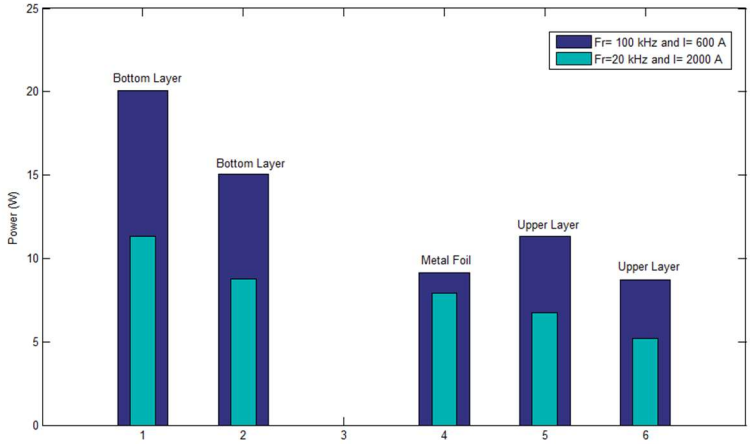

Figure 6: Comparison of powers in each layers (fr=20 kHz; I=2000A) and (fr=100 kHz; I=600A)

As we can see in the fig. 5, the ratio of power is about 45 percent when we choose 100 kHz as frequency. When we work with **100 kHz**, the power increase from 7 W to 64 W respectively with currents 200 A and 600 A. The total power (64 W) in the case 100 kHz and 600A is more important than the case 20 kHz and 2000A which is 39.95 W.

The simulated temperature at the surface (upper face) at frequency 100 kHz and current 600 A is shown in fig. 7. The composite plate is heated in 2s. The evolution of the temperature at the surface (upper face) is calculated for 60s. As we can see in the fig. 7, the temperature in the case with defect reached a maximum at t=6s and the temperature is the most important over almost the measurement period. The figure 8 shown the temporal evolution of the temperature at the middle of the metal foil.

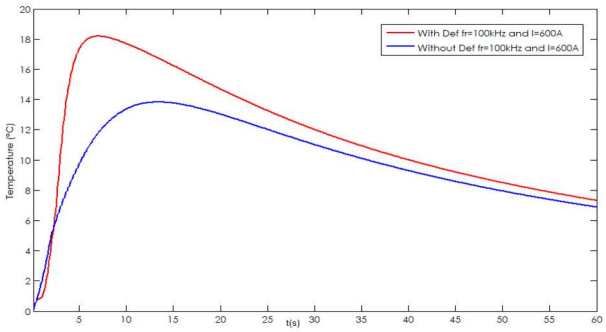

Figure 7: Temporal evolution of the temperature at the center of the defect upper face

Fig. 8 shows that the metal has heated well during the period when the generator is running. The temperature reached maximum at t=2s (heating time). The maximum of temperature is 35 °C. After shutting off the generator, the temperature at the middle of the metal foil begins to decrease. We can say that the power is well focused in the metal foil. This allows us to do well the inspection of the specimen.

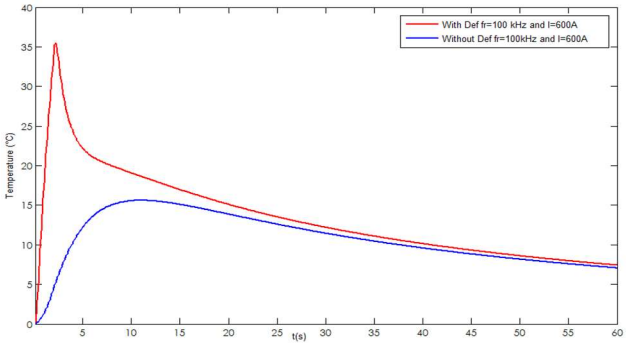

Figure 8: Temporal evolution of the temperature at the middle of the Metal Foil

3.1 Defect detection by absolute contrast image

Amplitude contrast technique consists of substraction between thermal images simulated on defective piece and healthy one, using Fast Fourier Transform (FFT). The non-null contrast areas on the resulting images allow for detection of defects. The Fourier transform is performed by the following well know formula:

$$\boldsymbol{F}(f) = \frac{1}{Nt}\sum_{i=0}^{N-1} T(i)\exp\left(-\frac{j2\pi fi}{Nt}\right) = Re(f) + Im(f) \qquad \text{(Eq. 15)}$$

$$A(f) = \sqrt{Re^2(f) + Im^2(f)}$$
$$C^{Amp} = A_{with_{Def}}(f) - A_{without_{Def}}(f) \qquad \text{(Eq. 16)}$$

Some images of amplitude contrast are shown in the fig. 9.

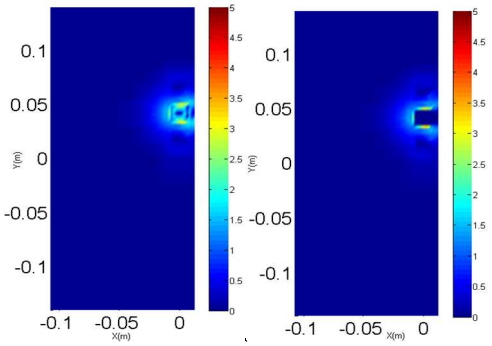

Figure 9: Amplitude Contrast Image FFT

4. Conclusion

Numerical investigations are used in this paper to evaluate the detectability of artificial defect metal foil on the interface of composite-adhesive bond. It was shown that the electromagnetic frequency and the current of the heating source are both significant parameters that have to be optimized in order to detect defects more clearly. Also, the thermal parameters (heating time, observation time, …) should be also optimized for should be also optimized for better resolution of the defects. In the future study, experimental investigations will be done by taking into account the parameters that are obtained from the simulation results.

Acknowledgments

This research was funded by NDTonAIR project from the European Union's Horizon 2020 research and innovation program under the Marie Sklodowska-Curie grant agreement No 722134-NDTonAIR.

References

[1] Bui H K, Wasselynck G, Trichet D and Berthiau G 2016 Study on flaw detectability of NDT induction thermography technique for laminated CFRP composites *Eur. Phys. J. Appl. Phys.* **73** 10902

[2] Yilmaz B, Jasiūnienė E and Mažeika L 2018 Evaluation of bonding quality by using ultrasonic waves *12th Eur. Conf. Non-Destructive Test. (ECNDT 2018), Gothenbg.* 2–4

[3] Bui H K, Berthiau G, Trichet D and Wasselynck G 2015 Inductive thermography nondestructive testing applied to carbon composite materials: multiphysics and multiscale modeling *8th Int. Conf. Electromagn. Process. Mater.* 403–6

[4] Ramdane B, Trichet D, Belkadi M, Saidi T and Fouladgar J 2010 3D numerical modeling of a new thermo-inductive NDT using pulse mode and pulsed phase methods *Eur. Phys. J. Appl. Phys.* **52** 23301

[5] Bui H K, Wasselynck G, Trichet D, Ramdane B, Berthiau G and Fouladgar J 2013 3-D modeling of thermo inductive non destructive testing method applied to multilayer composite *IEEE Trans. Magn.* **49** 1949–52

[6] Meunier G 2008 *The Finite Element Method for Electromagnetic Modeling* (ISTE Ltd, John Wiley & Sons Inc.)

[7] Bui H K, Senghor F D, Wasselynck G, Trichet D, Fouladgar J, Lee K and Berthiau G 2018 Characterization of Electrical Conductivity of Anisotropic CFRP Materials by Means of Induction Thermography Technique *IEEE Trans. Magn.* **54**